

Asteroseismology of Cool Stars

Daniel Huber^{1,2,3}

¹*NASA Ames Research Center, Moffett Field, CA 94035, USA*

²*SETI Institute, 189 Bernardo Avenue, Mountain View, CA 94043, USA*

³*Sydney Institute for Astronomy (SfA), School of Physics, University of Sydney, NSW 2006, Australia; dhuber@physics.usyd.edu.au*

Abstract. The measurement of oscillations excited by surface convection is a powerful method to study the structure and evolution of cool stars. *CoRoT* and *Kepler* have initiated a revolution in asteroseismology by detecting oscillations in thousands of stars from the main sequence to the red-giant branch, including a large number of exoplanet host stars. In this contribution I will review recent asteroseismic results, focusing in particular on the internal rotation of red giant stars and the impact of asteroseismology on the characterization of exoplanets.

1. Introduction

Stellar oscillations in cool stars are excited by turbulent convection in the outer layers (e.g. Houdek et al. 1999). Oscillation modes can be described by spherical harmonics with spherical degree l (the total number of node lines on the surface), azimuthal order $|m|$ (the number of node lines that cross the equator), and radial order n (the number of nodes from the surface to the center of the star). Radial pulsations are therefore expressed as $l = 0$, while $l > 0$ are non-radial pulsations. Modes with higher spherical degrees penetrate to shallower depths within the star (Figure .1).

Oscillation modes can furthermore be separated into pressure modes (p modes) and gravity modes (g modes). Pressure modes are acoustic waves propagating through the compression and decompression of gas, and pressure gradient acts as the restoring force. Gravity modes are pulsations due to the interplay of buoyancy and gravity, and buoyancy acts the restoring force. Gravity modes are damped where convection is unstable, and are therefore usually confined to the deep interior for cool stars. Pressure modes propagate in radiative zones, and hence are more easily excited to observational amplitudes on the surface.

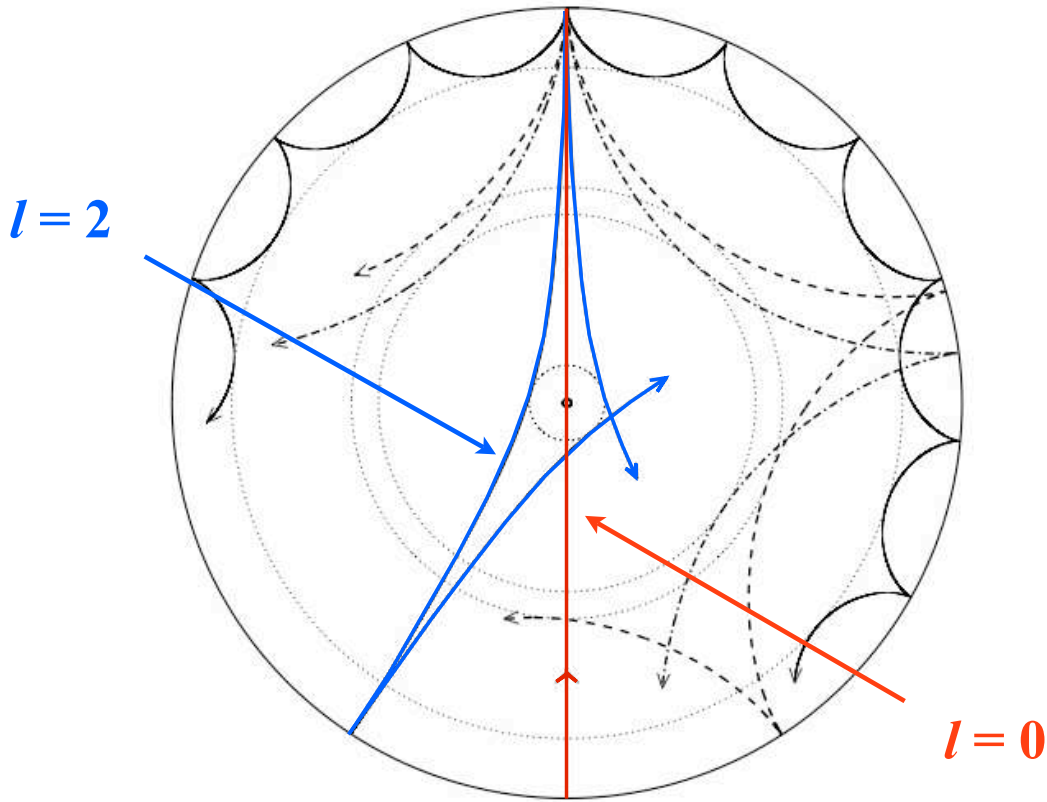


Figure .1: Schematic cross-section of a star illustrating the paths of modes with different spherical degrees l . Adapted from [Christensen-Dalsgaard \(2003\)](#).

Oscillation frequencies $\nu_{n,l}$ of high n and low l can be described by the asymptotic theory of stellar oscillations ([Vandakurov 1968](#); [Tassoul 1980](#); [Gough 1986](#)), which observationally can be approximated as follows:

$$\nu_{n,l} \approx \Delta\nu \left(n + \frac{1}{2}l + \epsilon \right) - \delta\nu_{0l}. \quad (1)$$

Here, the large frequency separation $\Delta\nu$ is the separation of modes of the same spherical degree l and consecutive radial order n , while modes with different degree l and same order n are separated by the small frequency separations $\delta\nu_{0l}$. In the asymptotic theory, $\Delta\nu$ can be shown to be equal to the inverse of twice the sound travel time through the stellar diameter ([Ulrich 1986](#); [Christensen-Dalsgaard 2003](#)):

$$\Delta\nu = \left(2 \int_0^R \frac{dr}{c} \right)^{-1}, \quad (2)$$

where c is the sound speed. Assuming adiabacity and an ideal gas $c \propto \sqrt{T/\mu}$ and $T \propto \mu M/R$, where μ is the mean molecular weight. Hence, Equation (2) can be expressed as (Kjeldsen & Bedding 1995):

$$\Delta\nu \propto \left(\frac{M}{R^3}\right)^{1/2}. \quad (3)$$

The large frequency separation is therefore a measure of the mean stellar density. The small frequency separations can be written as (Christensen-Dalsgaard 2003):

$$\delta\nu_{nl} = -(4l + 6) \frac{\Delta\nu}{4\pi^2\nu_{nl}} \int_0^R \frac{dc}{dr} \frac{dr}{r}. \quad (4)$$

The integral shows that $\delta\nu_{nl}$ is sensitive to sound-speed gradient in the stellar interior, which depends on the chemical composition profile. Hence, $\delta\nu_{nl}$ is sensitive to changes in the chemical composition during stellar evolution and thus stellar age. Equation (4) can be qualitatively understood by the fact that modes of different l travel to different depths within the star, and hence their frequency differences provide information about the radial structure.

An additional asteroseismic observable is the frequency of maximum power, ν_{\max} , which is related to the driving and damping of the modes. The frequency of maximum power has been suggested to scale with the acoustic cut-off frequency (Brown et al. 1991), which is the maximum frequency below which an acoustic mode can be reflected (Christensen-Dalsgaard 2003):

$$\nu_{\text{ac}} = \frac{c}{2H_p}. \quad (5)$$

Here, H_p is the pressure scale height. For an isothermal atmosphere $H_p = \frac{pR^2}{GM\rho}$, which combined with the ideal gas equation yields:

$$\nu_{\max} \propto \nu_{\text{ac}} \propto \frac{M}{R^2\sqrt{T_{\text{eff}}}}. \quad (6)$$

Hence, ν_{\max} is mainly a measure of the surface gravity of a star.

Measurements of ν_{\max} , $\Delta\nu$, $\delta\nu_{nl}$, or individual frequencies provide a powerful way to determine the stellar structure and fundamental stellar properties (such as radius and mass), which are otherwise difficult to measure for field stars. Validations of asteroseismic results with classical methods such as interferometry and eclipsing binary systems have shown good agreement within the typically quoted uncertainties (see, e.g., Belkacem 2012; Huber 2014, for recent reviews).

2. The Space Photometry Revolution of Asteroseismology

Early efforts to detect stellar oscillations used ground-based radial-velocity observations. The first confirmed detection dates back to Brown et al. (1991) in Procyon, followed by the first detection of regularly spaced frequencies in η Boo by Kjeldsen et al. (1995). The greatly improved sensitivity of Doppler velocities for detecting exoplanets enabled the detection

of oscillations in several nearby main sequence and subgiant stars such as β Hyi (Bedding et al. 2001; Carrier et al. 2001), α Cen A (Bouchy & Carrier 2001; Butler et al. 2004) and B (Carrier & Bourban 2003; Kjeldsen et al. 2005) as well as red giant stars such as ξ Hya (Frandsen et al. 2002) and ϵ Oph (De Ridder et al. 2006). At the same time, first space-based photometric observations led to detections with the Canadian space telescope *MOST* (Microvariability and Oscillations in Stars, Walker et al. 2003; Matthews 2007) in red giants (Barban et al. 2007; Kallinger et al. 2008) and Procyon (Guenther et al. 2008; Huber et al. 2011). Space-based observations were also performed using the startracker of the *WIRE* (Wide-Field Infrared Explorer) satellite (Schou & Buzasi 2001; Retter et al. 2003; Bruntt et al. 2005; Stello et al. 2008), the *SMEI* (Solar Mass Ejection Imager) experiment (Tarrant et al. 2007) and the Hubble Space Telescope (Edmonds & Gilliland 1996; Gilliland 2008; Stello & Gilliland 2009; Gilliland et al. 2011). In total, observational efforts prior to 2009 yielded detections in ~ 20 stars (see Figure .2).

A major breakthrough (and commonly referred to as the beginning of the space photometry revolution of asteroseismology) was achieved by the French-led *CoRoT* (Convection Rotation and Planetary Transits) satellite, which detected oscillations in a number of main sequence stars (e.g. Michel et al. 2008) and several thousands red giant stars (e.g. Hekker et al. 2009). Importantly, *CoRoT* showed that red giants oscillate in non-radial modes (De Ridder et al. 2009), which opened the door for detailed studies of the interior structure of red giants (see Section 3.).

The *Kepler* space telescope, launched in 2009, completed the revolution of cool-star asteroseismology by covering the low-mass H-R diagram with detections, including dwarfs cooler than the Sun (Chaplin et al. 2011) and over ten thousand red giants (Hekker et al. 2011; Stello et al. 2013). The larger number of red giants with detected oscillations is due to a combination of two effects: First, oscillation amplitudes increase with luminosity (Kjeldsen & Bedding 1995), making a detection easier at a given apparent magnitude. Second, the majority of *Kepler* targets were observed with 30-minute sampling, setting a limit of $\log g \lesssim 3.5$ since less evolved stars oscillate above the Nyquist frequency.

3. Probing the Cores of Red Giants

For evolved stars the p-mode and g-mode cavity can overlap, giving rise to so-called “mixed modes” (Dziembowski et al. 2001). Mixed modes contain contributions from g modes confined to the core, but unlike pure g modes can have low enough mode inertias to be observed at the surface. As opposed to p modes, g modes are theoretically predicted to be equally spaced in period. The coupling of p modes with g modes causes mixed modes to be shifted from their original frequency spacing (Aizenman et al. 1977), yielding multiple frequencies per radial order which are expected to be approximately equally spaced in period.

The detection of mixed $l = 1$ modes in red giants by *Kepler* (Bedding et al. 2010) led to several important discoveries in our understanding of the internal composition and rotation of giants. Following the observational confirmation of equal period spacings (Beck et al. 2011), Bedding et al. (2011) demonstrated that giants ascending the RGB and He-core burning red giants can be separated based on their mixed-mode period spacing (see also Mosser et al. 2011). Shortly after, Beck et al. (2012) showed that mixed modes are split into multiplets by rotation, and that frequency splittings for g-dominated mixed modes are substantially higher than for p-dominated mixed modes due radial differential rotation.

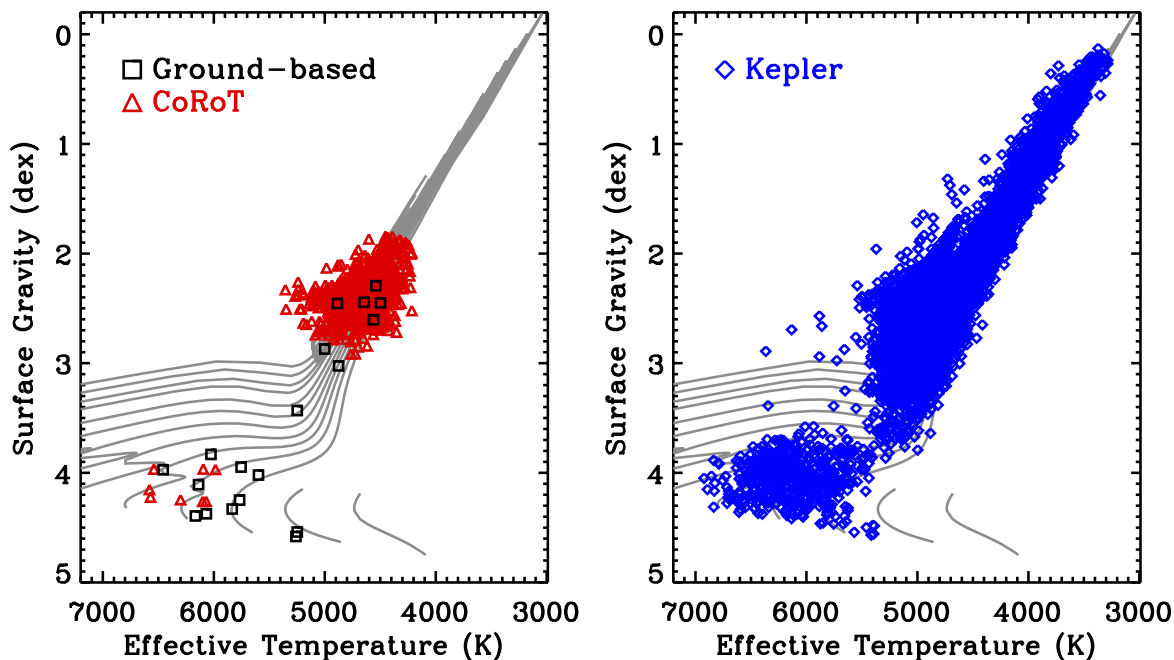


Figure .2: Stars with detected convection-driven oscillations in a $\log(g)$ - T_{eff} diagram. Left panel: Detections from ground- and space-based observations prior to 2009 (black squares) and by *CoRoT* (red triangles). Right panel: Detections by *Kepler* taken from [Huber et al. \(2014\)](#).

Core rotation rates were subsequently measured for hundreds of red giants, allowing an unprecedented view in the internal rotation evolution of evolved stars. Figure .3 shows seismically measured core rotation rates as a function of stellar radius for a sample of subgiants ([Deheuvels et al. 2014](#)) and red giants ([Mosser et al. 2013](#)). The data show that the cores spin up as stars evolve towards the RGB, followed by a gradual spin-down as stars evolve towards the He-core burning main sequence. Predicted core rotation rates in models are up to factors of 10–100 larger than observed ([Marques et al. 2013](#); [Cantiello et al. 2014](#)), pointing to a yet unidentified mechanism responsible for transporting angular momentum from the core to the envelope. The exquisite observational data promise significant advances in our theoretical understanding of the different roles of angular momentum transport mechanisms in stars (e.g. [Fuller et al. 2014](#)).

4. Asteroseismology of Exoplanet Host Stars

4.1 Characterization of Exoplanets

Transit and radial velocity surveys measure exoplanet properties relative to stellar properties, hence requiring a precise characterizations of host stars. Asteroseismology is a powerful tool to provide such characterizations in a systematic fashion. In particular, for observations

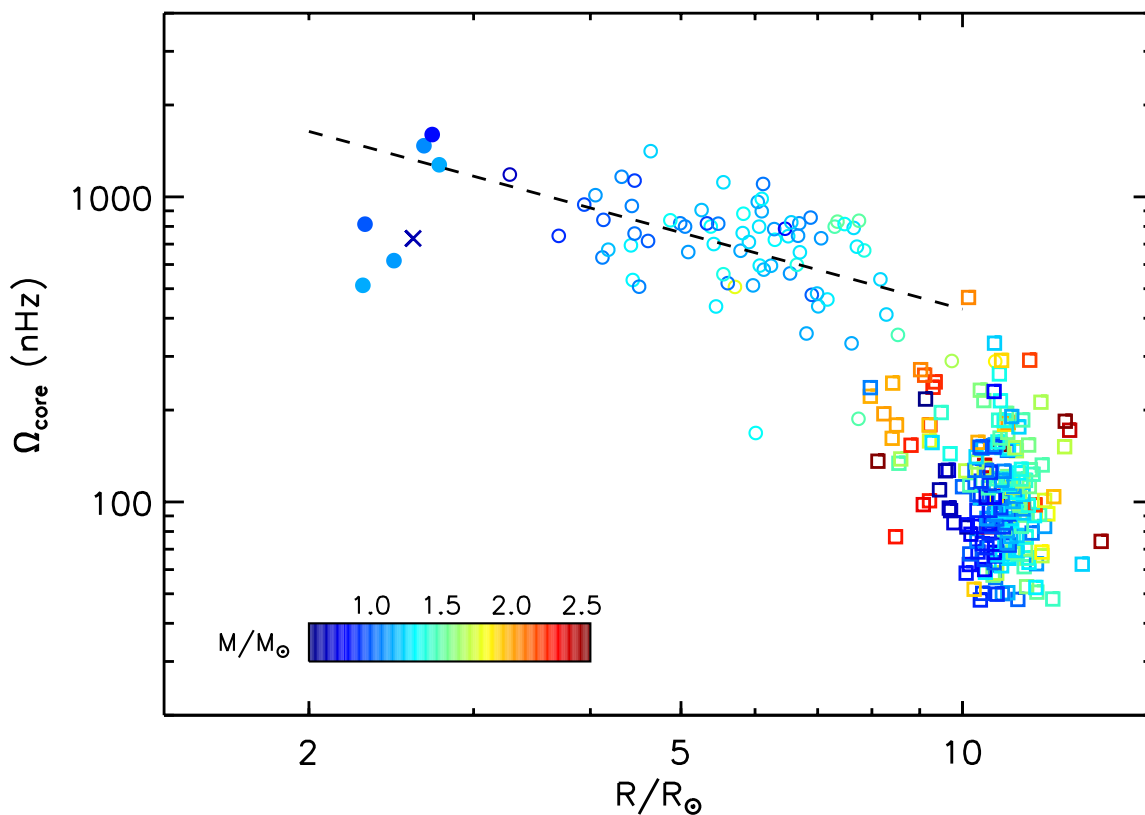


Figure .3: Core rotation frequency versus stellar radius for a sample of subgiants and red giants observed by *Kepler*. Circles mark RGB stars, squares He-core burning stars, and colors denote the stellar mass determined from asteroseismology. From [Deheuvels et al. \(2014\)](#).

with sufficiently high precision such as provided by *Kepler*, both planetary transits and stellar oscillations can be measured using the same data (Figure .4).

To date, nearly 80 *Kepler* host stars have been uniformly characterized using measurements of ν_{\max} and $\Delta\nu$, yielding precise ($\sim 3\%$) radii for over 100 exoplanet candidates (Figure .5, [Huber et al. 2013a](#)). For a smaller sample detailed frequency modeling has yielded even more precise radii, masses and ages with typical uncertainties of 1%, 2% and 10%, respectively (e.g. [Christensen-Dalsgaard et al. 2010](#); [Gilliland et al. 2013](#)). Efforts to derive precise and accurate seismic ages for more than 30 *Kepler* host stars are currently under way ([Davis et al, in prep](#); [Silva Aguirre et al., in prep](#)).

Comparisons with high-resolution spectroscopy for *Kepler* hosts showed that previous estimates of $\log g$ for evolved host stars were significantly overestimated, while characterizations for dwarfs generally show good agreement (Figure .5). The majority of *Kepler* host stars, however, still rely on photometric classifications from the Kepler Input Catalog ([Brown et al. 2011](#)), which have been suggested to suffer from biases for dwarfs ([Verner et al. 2011](#);

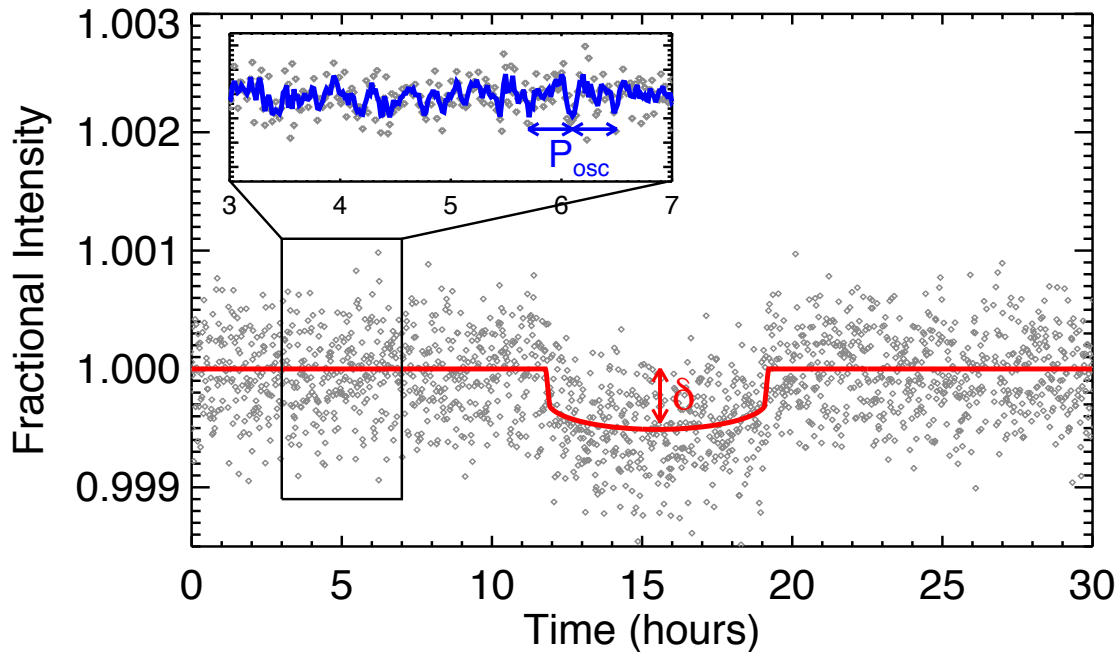


Figure 4: *Kepler* short-cadence light curve centered on a transit of Kepler-36c (Carter et al. 2012). The thick solid line shows the best-fitting transit model. The inset illustrates the oscillations of the host star. The transit depth δ yields the size of the planet relative to the size of the star, and the oscillation periods P_{osc} independently measure the size of the star.

Everett et al. 2013; Bastien et al. 2014). Asteroseismology will continue to play a key role to accurately quantify such biases through the calibration of less direct methods which are applicable to larger samples such as photometric flicker (Bastien et al. 2013) or spectroscopy.

4.2 Probing the Architecture of Exoplanet Systems

In addition to rotation periods, rotational splittings can be used to determine the line-of-sight inclination of the stellar rotation axis by measuring the relative heights of the $l(l+1)$ modes in each multiplet (Gizon & Solanki 2003). For dipole ($l=1$) modes, a doublet implies a high inclination (rotation axis perpendicular to the line of sight), while a triplet implies an intermediate inclination. Observing a single peak does not constrain the inclination since the star can either have a low inclination (pole-on) or show no splittings because of slow rotation.

Stellar inclinations are important for studying the architecture and dynamical history of transiting exoplanets by constraining the angle between the stellar spin axis and the planetary orbit axis (the obliquity). Since the presence of transits shows that the orbital axis is perpendicular to the line of sight, a low stellar inclination automatically implies

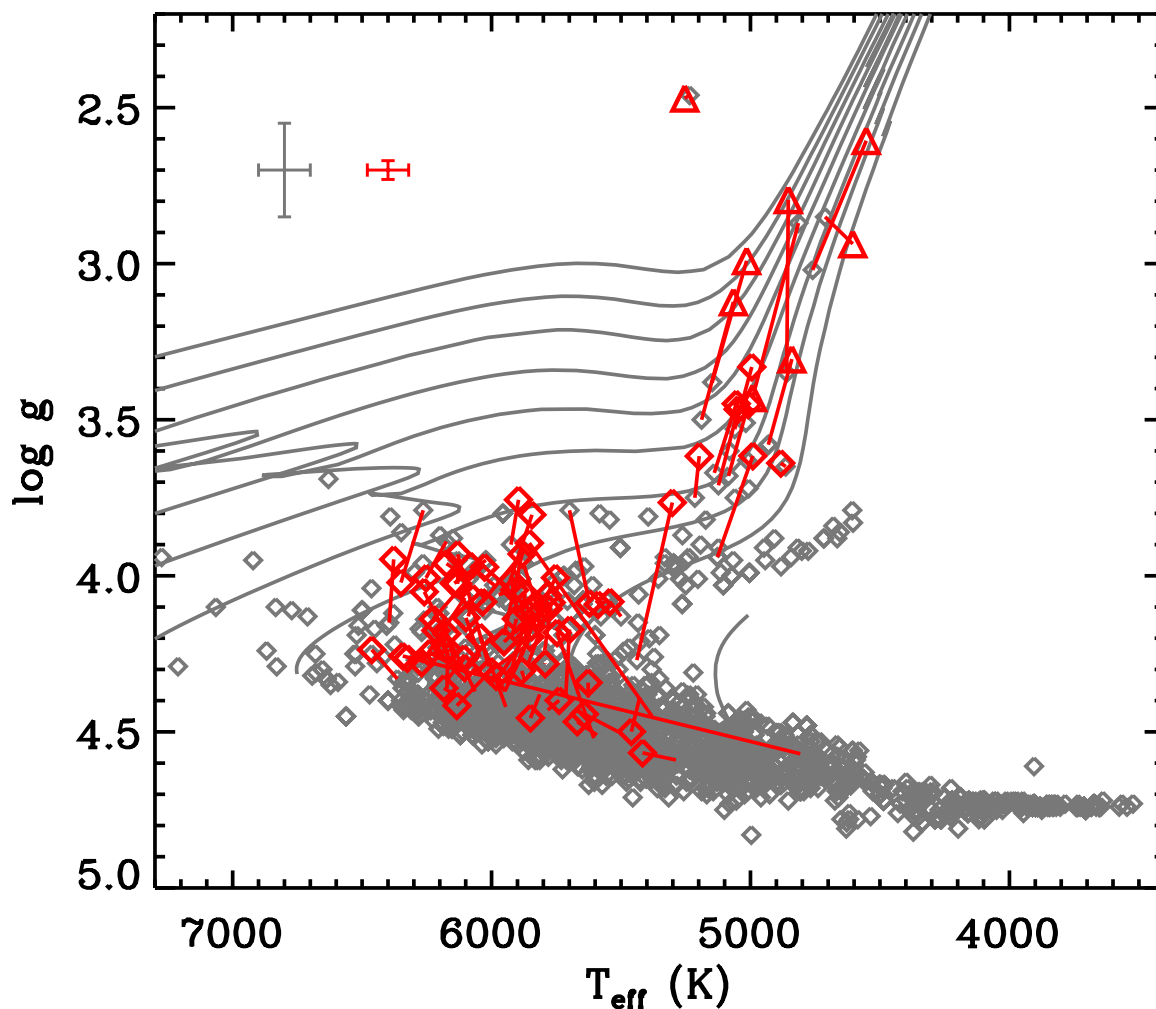


Figure 5: Surface gravity versus effective temperature for planet-candidate hosts in [Batalha et al. \(2013\)](#) (grey diamonds). Solar metallicity evolutionary tracks are shown as grey lines. Thick red symbols show positions of 77 host stars with asteroseismic detections using long-cadence (triangles) and short-cadence (diamonds) data, respectively. Red lines connect the revised positions to the values in [Batalha et al. \(2013\)](#). Typical error bars are shown in the top left side of the plot. From [Huber et al. \(2013a\)](#).

a misalignment of orbital plane and the equatorial plane of the star (a high obliquity)¹. High obliquities are frequently observed in stars hosting hot Jupiters (e.g. [Winn et al. 2010](#)), while stars hosting multiple coplanar planets have been observed to have low obliquities (e.g.

¹Conversely, an inclination near 90 degrees does not imply a low obliquity in the absence of a measurement of sky-projected stellar spin-orbit angle.

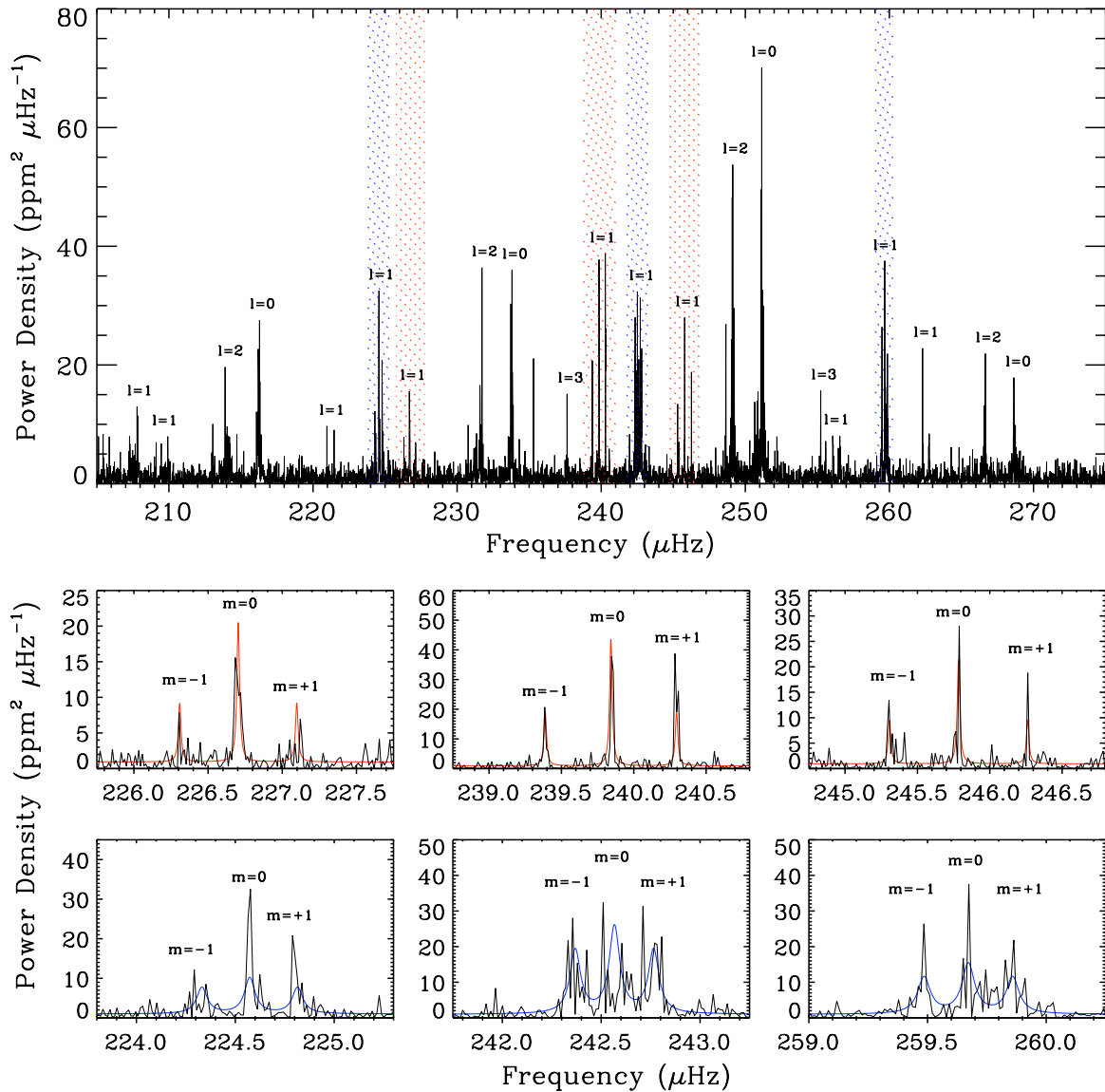


Figure .6: Top panel: Oscillation spectrum of Kepler-56. Gravity-dominated and pressure-dominated mixed dipole modes are highlighted as red and blue, respectively. Bottom panels: Close-up of dipole modes highlighted in the top panel. Each modes is split into a triplet by rotation, demonstrating that the spin axis of Kepler-56 is misaligned with the orbital axis of the two transiting planets. From [Huber et al. \(2013b\)](#).

[Sanchis-Ojeda et al. 2013](#)). This has been taken as evidence that the formation of hot Jupiters is related to dynamical interactions, rather than migrations through a protoplanetary disk.

High-precision photometry by *Kepler* and *CoRoT* have enabled asteroseismic stellar inclination measurements for several exoplanet systems ([Chaplin et al. 2013](#); [Gizon et al.](#)

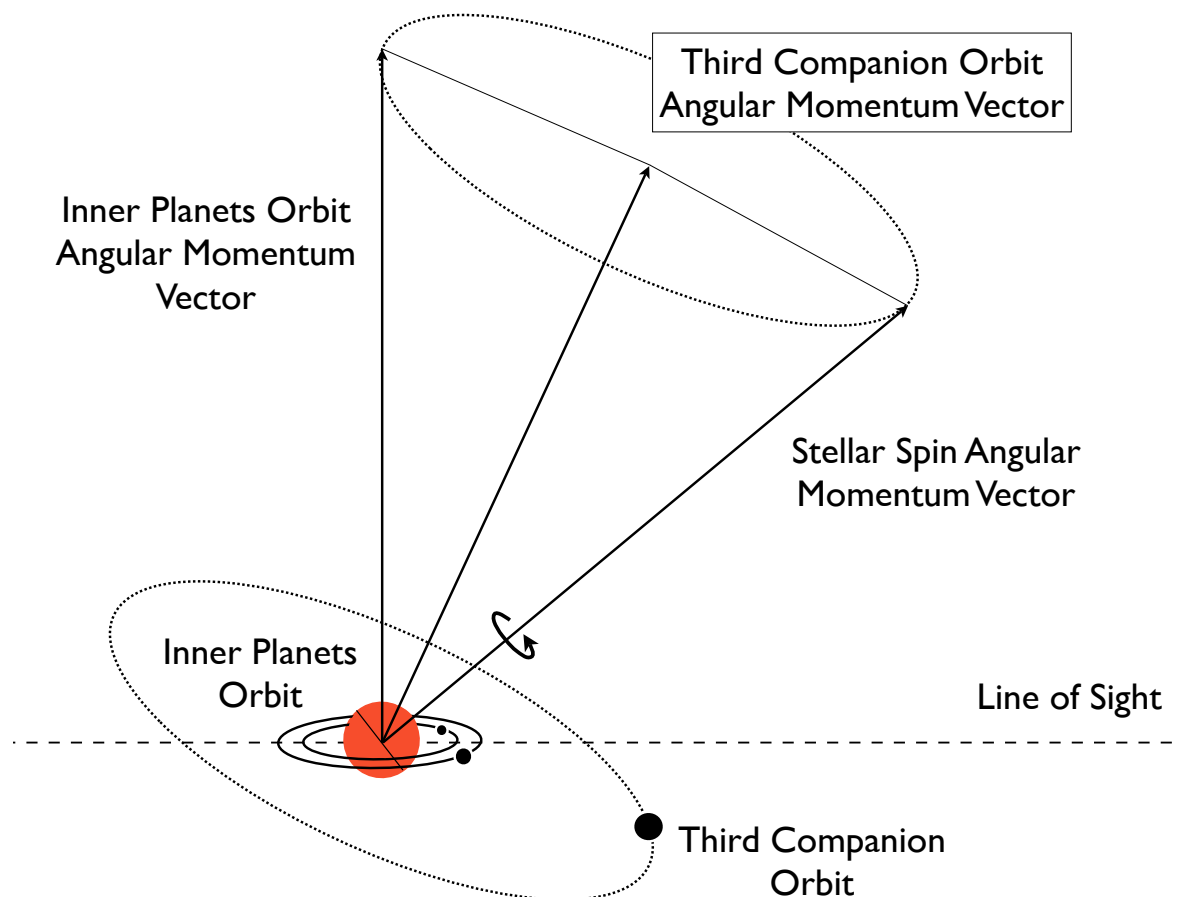


Figure .7: Graphical sketch of the Kepler-56 system. The torque of the outer companion causes a precession of the orbital axis of the inner transiting planets around the total angular momentum. The precession occurs at a different rate than the precession of spin axis of the host star, causing a periodic stellar spin-orbit misalignment. Sizes are not to scale. From [Huber et al. \(2013b\)](#).

2013; [Benomar et al. 2014](#); [Van Eylen et al. 2014](#); [Lund et al. 2014](#)). An intriguing example is Kepler-56, a red giant hosting two transiting planets initially confirmed through transit-timing variations ([Steffen et al. 2012](#)). The Kepler-56 power spectrum shows dipole modes which are split into triplets (Figure .6). Modeling the frequency triplets yielded an inclination of 47 ± 6 degrees, and demonstrated the first stellar spin-orbit misalignment in a multiplanet system ([Huber et al. 2013b](#)).

Follow-up radial velocity observations of Kepler-56 with Keck/HIRES revealed a long-term trend due to a massive companion on a wide orbit. Assuming a significant mutual inclination between the outer companion and the inner transiting planets, dynamical simulations showed that the misalignment can be explained by the precession of the orbital axis of the inner planets due to the torque of the wide companion (Figure .7), a scenario

which has previously been proposed theoretically (Mardling 2010; Kaib et al. 2011; Batygin 2012). Further simulations confirmed that the misalignment in Kepler-56 is consistent with a dynamical origin due to an inclined perturber (Li et al. 2014).

Kepler-56 demonstrated that spin-orbit misalignments are not confined to hot Jupiter systems, which has since also been suggested for the innermost planet of the 55 Cancri system based on Rossiter-McLaughlin observations (Bourrier & Hébrard 2014, but see also López-Morales et al., 2014). Further asteroseismic inclination measurements of exoplanet host stars, which are independent of the properties of planets and hence applicable to a wide range of systems, will reveal whether spin-orbit misalignments in multiplanet systems are common.

5. Conclusions

High-precision space-based photometry has triggered a revolution in asteroseismology of cool stars over the past few years. Highlights of recent asteroseismic discoveries presented in this review include the study of the internal rotation evolution of red giant stars and the precise characterization of the properties and architectures of exoplanet systems. Currently operating and planned space missions such as *K2* (Howell et al. 2014), *TESS* (Ricker et al. 2014) and *PLATO* (Rauer et al. 2014), as well as ground-based networks such as SONG (Grundahl et al. 2008) and LCOGT (Brown et al. 2013), promise a bright future for asteroseismic studies of cool stars and their planets over the coming decades.

Acknowledgements. Many thanks to Gerard van Belle and the LOC & SOC for a fantastic week in Flagstaff. Financial support was provided by NASA grant NNX14AB92G issued through the Kepler Participating Scientist Program and the Australian Research Councils Discovery Projects funding scheme (project number DEI40101364).

References

- Aizenman, M., Smeyers, P., & Weigert, A. 1977, *A&A*, 58, 41
- Barban, C., et al. 2007, *A&A*, 468, 1033
- Bastien, F. A., Stassun, K. G., Basri, G., & Pepper, J. 2013, *Nature*, 500, 427
- Bastien, F. A., Stassun, K. G., & Pepper, J. 2014, *ApJ*, 788, L9
- Batalha, N. M., et al. 2013, *ApJS*, 204, 24
- Batygin, K. 2012, *Nature*, 491, 418
- Beck, P. G., et al. 2011, *Science*, 332, 205
- . 2012, *Nature*, 481, 55
- Bedding, T. R., et al. 2001, *ApJ*, 549, L105
- . 2010, *ApJ*, 713, 935
- . 2011, *Nature*, 471, 608

- Belkacem, K. 2012, in SF2A-2012: Proceedings of the Annual meeting of the French Society of Astronomy and Astrophysics, ed. S. Boissier, P. de Laverny, N. Nardetto, R. Samadi, D. Valls-Gabaud, & H. Wozniak, 173–188
- Benomar, O., Masuda, K., Shibahashi, H., & Suto, Y. 2014, PASJ
- Bouchy, F., & Carrier, F. 2001, A&A, 374, L5
- Bourrier, V., & Hébrard, G. 2014, A&A, 569, A65
- Brown, T. M., Gilliland, R. L., Noyes, R. W., & Ramsey, L. W. 1991, ApJ, 368, 599
- Brown, T. M., Latham, D. W., Everett, M. E., & Esquerdo, G. A. 2011, AJ, 142, 112
- Brown, T. M., et al. 2013, PASP, 125, 1031
- Bruntt, H., Kjeldsen, H., Buzasi, D. L., & Bedding, T. R. 2005, ApJ, 633, 440
- Butler, R. P., Bedding, T. R., Kjeldsen, H., McCarthy, C., O’Toole, S. J., Tinney, C. G., Marcy, G. W., & Wright, J. T. 2004, ApJ, 600, L75
- Cantiello, M., Mankovich, C., Bildsten, L., Christensen-Dalsgaard, J., & Paxton, B. 2014, ApJ, 788, 93
- Carrier, F., & Bourban, G. 2003, A&A, 406, L23
- Carrier, F., et al. 2001, A&A, 378, 142
- Carter, J. A., et al. 2012, Science, 337, 556
- Chaplin, W. J., et al. 2011, Science, 332, 213
- . 2013, ApJ, 766, 101
- Christensen-Dalsgaard. 2003, Lecture Notes, Aarhus University; <http://astro.phys.au.dk/jcd/oscilnotes/>
- Christensen-Dalsgaard, J., et al. 2010, ApJ, 713, L164
- De Ridder, J., Barban, C., Carrier, F., Mazumdar, A., Eggenberger, P., Aerts, C., Deruyter, S., & Vanautgaerden, J. 2006, A&A, 448, 689
- De Ridder, J., et al. 2009, *Nature*, 459, 398
- Deheuvels, S., et al. 2014, A&A, 564, A27
- Dziembowski, W. A., Gough, D. O., Houdek, G., & Sienkiewicz, R. 2001, MNRAS, 328, 601
- Edmonds, P. D., & Gilliland, R. L. 1996, ApJ, 464, L157
- Everett, M. E., Howell, S. B., Silva, D. R., & Szkody, P. 2013, ApJ, 771, 107
- Frandsen, S., et al. 2002, A&A, 394, L5
- Fuller, J., Lecoanet, D., Cantiello, M., & Brown, B. 2014, ApJ, in press (arXiv:1409.6835)
- Gilliland, R. L. 2008, AJ, 136, 566
- Gilliland, R. L., McCullough, P. R., Nelan, E. P., Brown, T. M., Charbonneau, D., Nutzman, P., Christensen-Dalsgaard, J., & Kjeldsen, H. 2011, ApJ, 726, 2

- Gilliland, R. L., et al. 2013, *ApJ*, 766, 40
- Gizon, L., & Solanki, S. K. 2003, *ApJ*, 589, 1009
- Gizon, L., et al. 2013, *Proceedings of the National Academy of Science*, 110, 13267
- Gough, D. O. 1986, in *Hydrodynamic and Magnetodynamic Problems in the Sun and Stars*, ed. Y. Osaki (Uni. of Tokyo Press), 117
- Grundahl, F., Christensen-Dalsgaard, J., Kjeldsen, H., Frandsen, S., Arentoft, T., Kjaergaard, P., & Jørgensen, U. G. 2008, in *IAU Symposium*, Vol. 252, *IAU Symposium*, ed. L. Deng & K. L. Chan, 465–466
- Guenther, D. B., et al. 2008, *ApJ*, 687, 1448
- Hekker, S., et al. 2009, *A&A*, 506, 465
- . 2011, *MNRAS*, 414, 2594
- Houdek, G., Balmforth, N. J., Christensen-Dalsgaard, J., & Gough, D. O. 1999, *A&A*, 351, 582
- Howell, S. B., et al. 2014, *PASP*, 126, 398
- Huber, D. 2014, arXiv:1404.7501
- Huber, D., et al. 2011, *ApJ*, 731, 94
- . 2013a, *ApJ*, 767, 127
- . 2013b, *Science*, 342, 331
- . 2014, *ApJS*, 211, 2
- Kaib, N. A., Raymond, S. N., & Duncan, M. J. 2011, *ApJ*, 742, L24
- Kallinger, T., et al. 2008, *Communications in Asteroseismology*, 153, 84
- Kjeldsen, H., & Bedding, T. R. 1995, *A&A*, 293, 87
- Kjeldsen, H., Bedding, T. R., Viskum, M., & Frandsen, S. 1995, *AJ*, 109, 1313
- Kjeldsen, H., et al. 2005, *ApJ*, 635, 1281
- Li, G., Naoz, S., Valsecchi, F., Johnson, J. A., & Rasio, F. A. 2014, *ApJ*, 794, 131
- López-Morales, M., et al. 2014, *ApJ*, 792, L31
- Lund, M. N., et al. 2014, *A&A*, 570, A54
- Mardling, R. A. 2010, *MNRAS*, 407, 1048
- Marques, J. P., et al. 2013, *A&A*, 549, A74
- Matthews, J. M. 2007, *Communications in Asteroseismology*, 150, 333
- Michel, E., et al. 2008, *Science*, 322, 558
- Mosser, B., et al. 2011, *A&A*, 532, A86
- . 2013, *A&A*, 550, A126
- Rauer, H., et al. 2014, *Experimental Astronomy*

- Retter, A., Bedding, T. R., Buzasi, D. L., Kjeldsen, H., & Kiss, L. L. 2003, *ApJ*, 591, L151
- Ricker, G. R., et al. 2014, in *Society of Photo-Optical Instrumentation Engineers (SPIE) Conference Series*, Vol. 9143, *Society of Photo-Optical Instrumentation Engineers (SPIE) Conference Series*, 20
- Sanchis-Ojeda, R., et al. 2013, *ApJ*, 775, 54
- Schou, J., & Buzasi, D. L. 2001, in *ESA Special Publication*, Vol. 464, *SOHO 10/GONG 2000 Workshop: Helio- and Asteroseismology at the Dawn of the Millennium*, ed. A. Wilson & P. L. Pallé, 391–394
- Steffen, J. H., et al. 2012, *MNRAS*, 421, 2342
- Stello, D., Bruntt, H., Preston, H., & Buzasi, D. 2008, *ApJ*, 674, L53
- Stello, D., & Gilliland, R. L. 2009, *ApJ*, 700, 949
- Stello, D., et al. 2013, *ApJ*, 765, L41
- Tarrant, N. J., Chaplin, W. J., Elsworth, Y., Sreckley, S. A., & Stevens, I. R. 2007, *MNRAS*, 382, L48
- Tassoul, M. 1980, *ApJS*, 43, 469
- Ulrich, R. K. 1986, *ApJ*, 306, L37
- Van Eynen, V., et al. 2014, *ApJ*, 782, 14
- Vandakurov, Y. V. 1968, *Soviet Ast.*, 11, 630
- Verner, G. A., et al. 2011, *MNRAS*, 415, 3539
- Walker, G., et al. 2003, *PASP*, 115, 1023
- Winn, J. N., Fabrycky, D., Albrecht, S., & Johnson, J. A. 2010, *ApJ*, 718, L145